# miR-34b/c Regulates Wnt1 and Enhances Mesencephalic Dopaminergic Neuron Differentiation

De Gregorio, Roberto

2018-04-10

De Gregorio , R , Pulcrano , S , De Sanctis , C , Volpicelli , F , Guatteo , E , von Oerthel , L , Latagliata , E C , Esposito , R , Piscitelli , R M , Perrone-Capano , C , Costa , V , Greco , D , Puglisi-Allegra , S , Smidt , M P , di Porzio , U , Caiazzo , M , Mercuri , N B , Li , M & Bellenchi , G C 2018 , ' miR-34b/c Regulates Wnt1 and Enhances Mesencephalic Dopaminergic Neuron Differentiation ' , Stem cell reports , vol. 10 , no. 4 , pp. 1237-1250 . https://doi.org/10.1016/j.st

http://hdl.handle.net/10138/239260
https://doi.org/10.1016/j.stemcr.2018.02.006

Please cite this article in press as: De Gregorio et al., miR-34b/c Regulates *Wnt1* and Enhances Mesencephalic Dopaminergic Neuron Differentiation, Stem Cell Reports (2018), https://doi.org/10.1016/j.stemcr.2018.02.006

Stem Cell Reports
**Article**

ISSCR

OPEN ACCESS

# miR-34b/c Regulates *Wnt1* and Enhances Mesencephalic Dopaminergic Neuron Differentiation

Roberto De Gregorio,[1,11,12] Salvatore Pulcrano,[1,3,12] Claudia De Sanctis,[1,2] Floriana Volpicelli,[1,3] Ezia Guatteo,[8,9] Lars von Oerthel,[4] Emanuele Claudio Latagliata,[8] Roberta Esposito,[1] Rosa Maria Piscitelli,[8,9] Carla Perrone-Capano,[1,3] Valerio Costa,[1] Dario Greco,[5] Stefano Puglisi-Allegra,[8] Marten P. Smidt,[4] Umberto di Porzio,[1] Massimiliano Caiazzo,[6] Nicola Biagio Mercuri,[8,10] Meng Li,[7] and Gian Carlo Bellenchi[1,*]

[1]Institute of Genetics and Biophysics, "Adriano Buzzati Traverso", CNR, 80131 Naples, Italy
[2]Neuromed IRCCS, 86077 Pozzilli (IS), Italy
[3]Deparment of Pharmacy, University of Naples Federico II, 80131 Naples, Italy
[4]Swammerdam Institute for Life Sciences, University of Amsterdam, 1090 GE Amsterdam, the Netherlands
[5]Institute of Biotechnology, University of Helsinki, 00014 Helsinki, Finland
[6]Department of Pharmaceutics, Utrecht Institute for Pharmaceutical Sciences, 3584 CG Utrecht, the Netherlands
[7]Neuroscience and Mental Health Research Institute, School of Medicine and School of Bioscience, Cardiff University, Cardiff CF24 4HQ, UK
[8]Fondazione Santa Lucia IRCCS, 00143 Rome, Italy
[9]Parthenope University, Department of Motor Science and Wellness, 80133 Naples, Italy
[10]University of Tor Vergata, Department of Systems Medicine, 00133 Rome, Italy
[11]Present address: Department of Molecular Pharmacology, Albert Einstein College of Medicine, New York, NY 10461, USA
[12]Co-first author
*Correspondence: giancarlo.bellenchi@igb.cnr.it
https://doi.org/10.1016/j.stemcr.2018.02.006

## SUMMARY

The differentiation of dopaminergic neurons requires concerted action of morphogens and transcription factors acting in a precise and well-defined time window. Very little is known about the potential role of microRNA in these events. By performing a microRNA-mRNA paired microarray screening, we identified miR-34b/c among the most upregulated microRNAs during dopaminergic differentiation. Interestingly, miR-34b/c modulates *Wnt1* expression, promotes cell cycle exit, and induces dopaminergic differentiation. When combined with transcription factors ASCL1 and NURR1, miR-34b/c doubled the yield of transdifferentiated fibroblasts into dopaminergic neurons. Induced dopaminergic (iDA) cells synthesize dopamine and show spontaneous electrical activity, reversibly blocked by tetrodotoxin, consistent with the electrophysiological properties featured by brain dopaminergic neurons. Our findings point to a role for miR-34b/c in neuronal commitment and highlight the potential of exploiting its synergy with key transcription factors in enhancing *in vitro* generation of dopaminergic neurons.

## INTRODUCTION

MicroRNAs (miRNAs) are a class of small non-coding single-strand RNA (~22 nucleotides) acting as post-transcriptional regulators of gene expression (Bartel and Chen, 2004). They are crucial players in several aspects of brain development such as neurogenesis, neuronal maturation, synapse formation, axon guidance, and neuronal plasticity (Kapsimali et al., 2007; McNeill and Van Vactor, 2012). Disruption of miRNA biogenesis by genetic deletion of *Dicer* has been a widely used strategy to investigate the role of miRNAs in neurodevelopmental processes (Cuellar et al., 2008; Davis et al., 2008; Kawase-Koga et al., 2009). Cell-type-specific deletion of miRNAs involved in mesencephalic dopaminergic (mDA) neurons causes progressive loss of these cells (Kim et al., 2007), suggesting a pivotal role for miRNA in mDA neuron formation, survival, and function. A number of laboratories attempted the identification of miRNAs involved in mDA neuron differentiation and diseases affecting the mDA system such as Parkinson's disease (Kim et al., 2007; Miñones-Moyano et al., 2011; Saba et al., 2012; Tobon et al., 2012; Yang et al., 2012).

Interestingly, recent works highlighted the importance of miRNAs, miR-135a2 in particular, in determining midbrain size and the allocation of prospective mDA precursors by modulating the extent of the Wnt signaling. The latter takes place through direct regulation of *Lmx1b*, in a context where excessive Wnt signaling has been shown to lead to improper mDA specification (Joksimovic and Awatramani, 2014; Nouri et al., 2015). Thus, manipulation of Wnt signaling has become an attractive strategy to define new *in vitro* differentiation protocols to increase the fraction of mDA neurons.

In addition, miRNAs are also emerging as possible components in both direct and indirect cell reprogramming strategies. Specific miRNAs are able to potentiate transcription factor-mediated conversion of mouse embryonic fibroblasts (MEFs) into induced pluripotent stem cells (Judson et al., 2009; Subramanyam et al., 2011). While two miRNAs, miR-9/9* and miR-124, are able to convert fibroblasts into neurons (Yoo et al., 2011) or into a specific subset of neurons if combined with defined transcription factors (Victor et al., 2014), to date, the ability of miRNAs to enhance dopaminergic

Please cite this article in press as: De Gregorio et al., miR-34b/c Regulates *Wnt1* and Enhances Mesencephalic Dopaminergic Neuron Differentiation, Stem Cell Reports (2018), https://doi.org/10.1016/j.stemcr.2018.02.006

(DA) transdifferentiation (Caiazzo et al., 2011) is largely unexplored.

MiR-34b-5p and miR-34c-5p (hereafter named miR-34b/c) belong to a large family of miRNAs that include miR-34a-5p and the miR-449 cluster (449a-5p, 449b-5p, and 449c-5p). They all share the same seed sequence and are considered as having overlapping roles. More recently it has been shown that miR-34a/b/c share only 20% of targets, suggesting that individual miR-34 family members exert largely unique roles (Navarro and Lieberman, 2015). Interestingly, miR-34b/c expression was altered in Parkinson's disease (PD), where it was found significantly downregulated in brain areas of PD patients with different degrees of pathology, prior to the appearance of motor dysfunction (Miñones-Moyano et al., 2011).

In this work, we identified the miR-34b/c cluster as an additional modulator of the Wnt signaling pathway. Enforced expression of miR-34b/c significantly increases *in vitro* differentiation of DA neurons. We show that miR-34b/c is able to directly bind the *Wnt1 3′UTR* and to regulate its expression. Consistently, overexpression of miR-34b/c leads to reduction of *Wnt1* and *Lmx1b* in DA-differentiated mouse embryonic stem cells (mESCs). In combination with the induced dopaminergic (iDA)-specific transcription factors ASCL1 and NURR1 (Caiazzo et al., 2011), miR-34b/c doubles the transdifferentiation efficiency, leading to the generation of functional iDA neurons with characteristic electrophysiological properties.

## RESULTS

### Modulation of the Wnt Pathway during mDA Neuron Differentiation

To investigate the roles of miRNAs in DA neuron fate specification, we performed a microarray screen and measured the expression of both mRNAs and miRNAs during DA differentiation of epiblast-derived stem cells (epiSCs) using a monolayer differentiation (MD) method developed previously (Jaeger et al., 2011). As a control, the same cells were differentiated in the basal condition without Sonic Hedgehog (SHH) and fibroblast growth factor 8 (FGF8), leading to the production of mostly GABAergic neurons. Samples were harvested at day 9 and day 14 MD (Figure 1A) and the RNAs processed for gene expression for mRNAs and miRNAs by microarray. To evaluate the activation of specific differentiation programs, we analyzed the expression of genes involved in developmental fate specifications and neuronal maturation at day 9 and day 14 MD in DA and control samples. In SHH/FGF8-treated cells mDA-associated transcripts were upregulated at both day 9 and day 14 while the expression of markers for GABAergic, glutamatergic, or adrenergic neurons were downregulated. Furthermore, we did not find any difference between the two conditions in the expression of markers for anterior/posterior identity (Figure 1B). The induction of DA fate was further confirmed by following the expression of selected mDA markers such as *Th*, *Nurr1*, *Pitx3*, *Dmrt5*, *Foxa2a*, and *Lmx1a*. All these gene markers showed a robust upregulation at the end the differentiation protocol in cultures treated with SHH and FGF8 (Figure 1C). In contrast, general neuronal markers, such as *Tubb3*, *Ascl1*, *Map2*, and *Ngn2*, have a similar expression profile in both DA and control conditions (Figure 1D). Consistent with the transcript analysis, immunostaining for tyrosine hydroxylase (TH) and GFP (for PITX3-GFP) at the end of the differentiation protocol confirmed the generation of DA neurons (Figure 1E).

By comparing gene expression profiles at day 9 and day 14 MD in SHH/FGF8-treated samples (david.ncifcrf.gov) (Huang et al., 2007a), we noticed that the Wnt signaling pathway becomes one of the most affected KEGG (Kyoto Encyclopedia of Genes and Genomes) pathways along the DA differentiation (Figure 2A).

We have previously performed microarray screening comparing the floor plate (ventral midbrain, mDA) versus basal plate (non-DA) transcripts at three embryonic time points: embryonic day 9.5 (E9.5), E10.5, and E12.5 (Gennet et al., 2011). Reanalysis of this dataset revealed that only five Wnts (*Wnt1*, *Wnt5a*, *Wnt5b*, *Wnt7a*, and *Wnt9a*) are expressed at E9.5 but their expression decreases progressively until E12.5 (Figure 2B). The same genes were also affected in our microarray dataset, from day 9 and day 14 MD. By comparing epiSC differentiated toward an mDA phenotype with cells differentiated in control condition, giving rise to mainly GABAergic neurons, we found by qPCR that *Wnt5a*, *Wnt5b*, and *Wnt9a* increased during mDA differentiation while *Wnt1* was maintained at a lower level (Figure 2C). The reduction of *Wnt1* was paralleled by that of *Lmx1b* (Figure 2C), a transcription factor known to be involved in early stages of MHB formation (Guo et al., 2007) and was recently associated with *Wnt1* as part of a regulatory loop together with miR-135a2-5p (Anderegg et al., 2013). Interestingly, the analysis of the array data show that most of the genes that positively affect the Wnt signaling were downregulated at day 14 MD, while some known inhibitors of the Wnt pathway, such as *Gsk3β* or *Ctnnbip1*, were upregulated (Figure 2D and scheme in Figure 2E). Together, these data suggest that the regulation of Wnt signaling during DA differentiation is needed to achieve proper generation of mDA neurons.

### Mir-34b/c Targets *Wnt1* and Is Enriched in Purified PITX3-GFP$^+$ mDA Neurons

To test the hypothesis that negative regulation of the Wnt pathway could be achieved through the action of miRNAs, we screened miRNA-specific array data for miRNAs upregulated during DA differentiation. By using an available

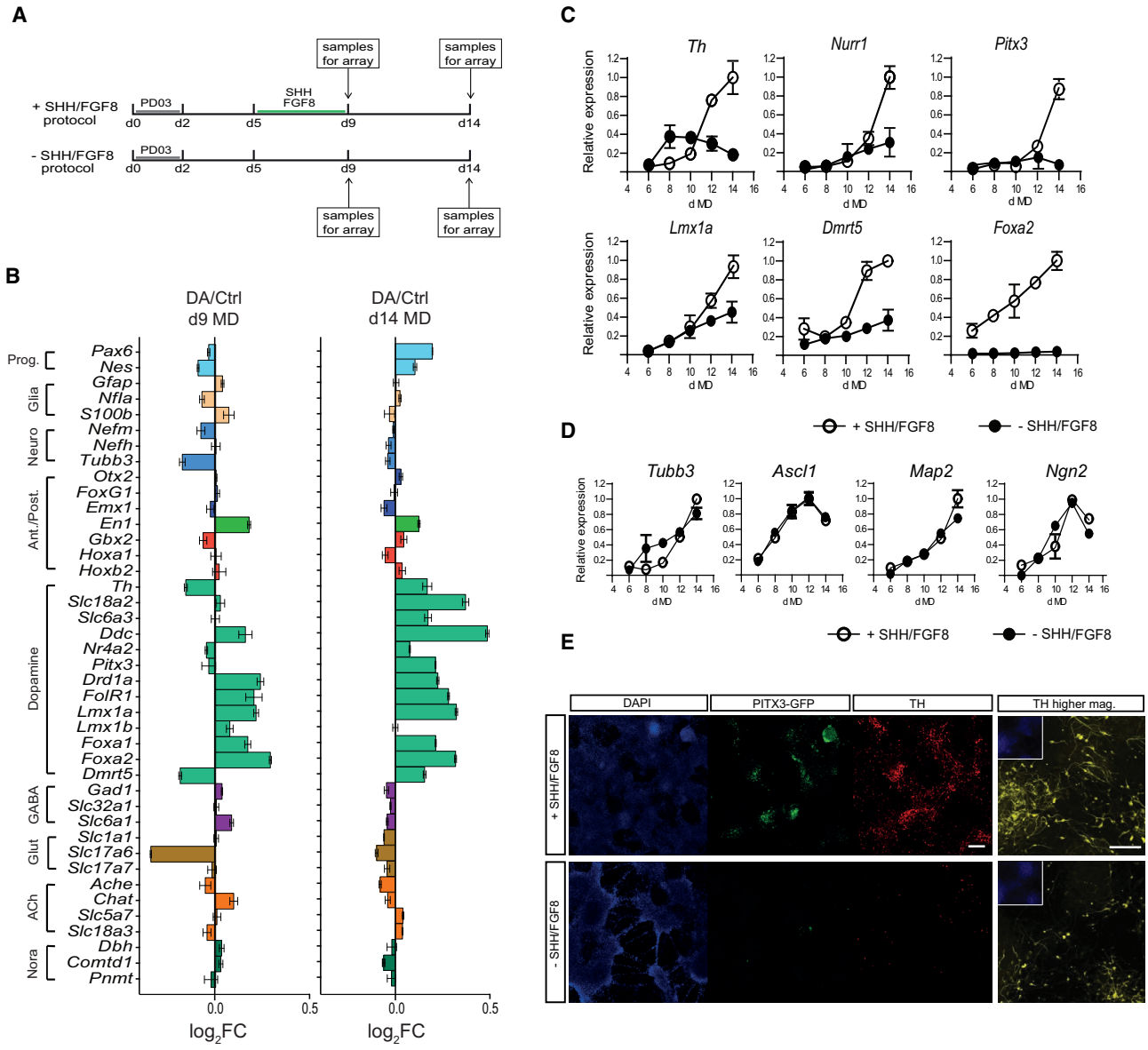


**Figure 1. Profiling of epiSC-Derived Dopaminergic Cells**

(A) Schematic representation of the protocols used to profile miRNAs and mRNAs expression during DA differentiation of mouse epiSCs. RNA samples were harvested in triplicate on day 9 MD and day 14 MD.

(B) The expression of genes representative for specific developmental fate and for different neuronal populations is shown at day 9 and day 14 MD. Data are presented as log(DA/Ctrl).

(C and D) qPCR for the expression of (C) DA-specific markers or (D) general neuronal markers over the differentiation protocol from day 6 MD to day 14 MD. All qPCR data have been normalized to the average of the reference gene *Hmbs*. The highest value for each gene (among both +SHH/FGF8 and −SHH/FGF8 samples) was set to 1. All other values are expressed as a ratio of 1. Data represent mean ± SEM from three independent experiments.

(E) *Pitx3-GFP* epiSC at day 14 MD differentiated in the presence (+) or absence (−) of SHH and FGF8 and immunostained for TH (red) and GFP (green) expression. High-magnification images for TH (yellow) with DAPI (blue) counterstain. Scale bars represent 200 μm and 100 μm, respectively, for the low- and high-magnification images.

miRNA target prediction tool (*targetscan.org/mmu_71/*) (Agarwal et al., 2015) we scanned for all miRNAs upregulated both at day 9 and at day 14, in SHH/FGF8-treated cells compared with controls, which are predicted to bind to the 3′ UTR of downregulated genes in the Wnt signaling pathway. MiR-34b/c and miR-148a-3p both scored in

Please cite this article in press as: De Gregorio et al., miR-34b/c Regulates *Wnt1* and Enhances Mesencephalic Dopaminergic Neuron Differentiation, Stem Cell Reports (2018), https://doi.org/10.1016/j.stemcr.2018.02.006

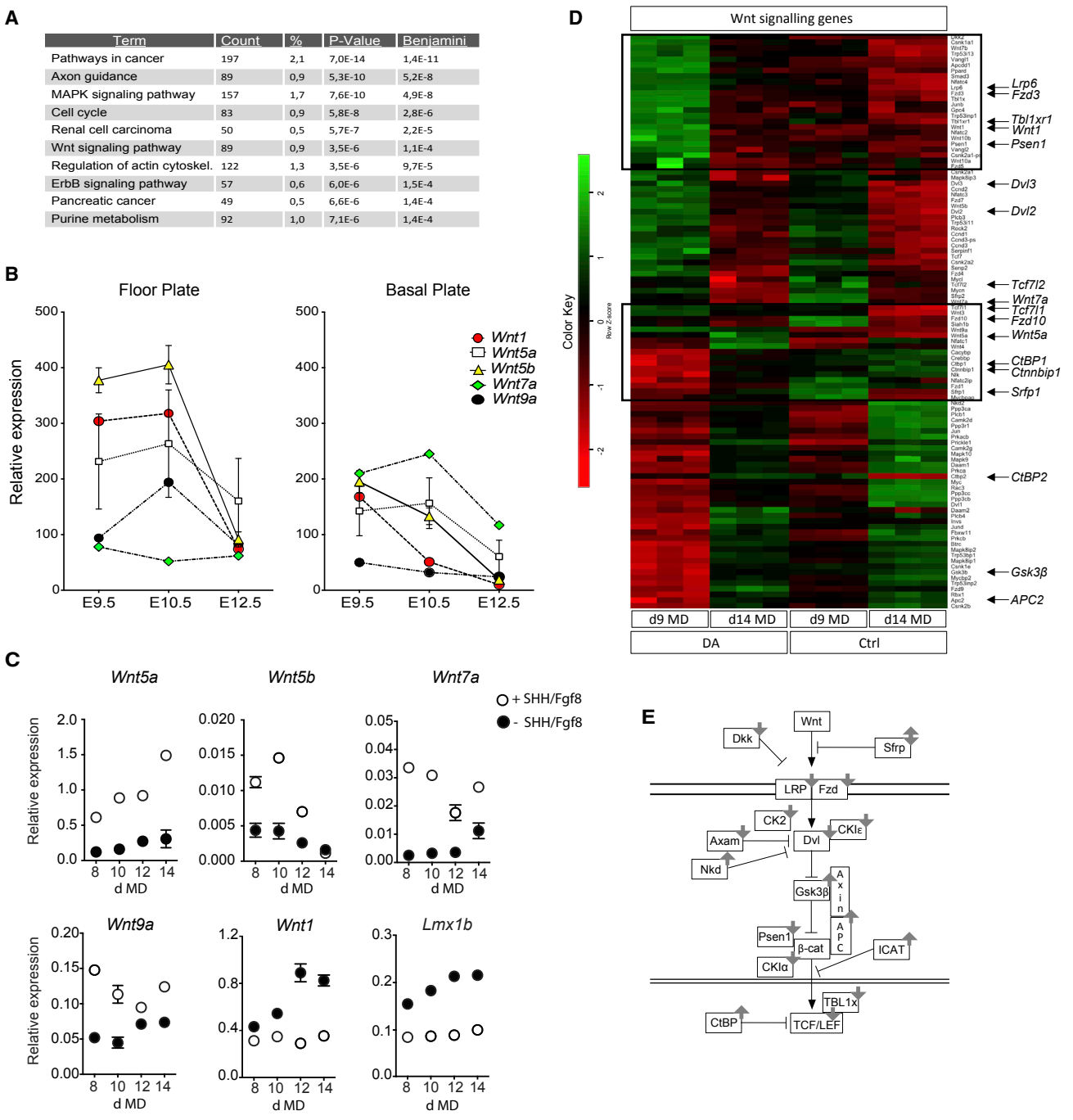


**Figure 2. The Wnt Pathway during mDA Differentiation of epiSCs**

(A) Top ten categories of KEGG pathways associated with differentially expressed genes between day 9 MD and day 14 MD of the dopaminergic differentiation protocol (+SHH/FGF8). The p values were calculated using hypergeometric test and corrected by Benjamini-Hochberg adjustment.

(B) Relative expression of the most expressed Wnt genes in floor plate and basal plate during embryonic development, from E9.5 to E12.5.

(C) qPCR for the expression of *Wnt5a*, *Wnt5b*, *Wnt7a*, *Wnt9a*, *Wnt1*, and *Lmx1b* during epiSC differentiation into DA (+SHH/FGF8) or control (−SHH/FGF8) neurons. Data represent mean ± SEM from three independent experiments.

*(legend continued on next page)*

our list with 18 and 13 predicted binding sites, respectively (Figure 3A), and were predicted also to directly target *Wnt1* (Figure 3B).

*Pitx3-GFP* is a mouse line in which the mDA neurons are exclusively labeled by the knockin GFP reporter (Zhao et al., 2004). Interestingly both miR-34b/c and miR-148a-3p were enriched in fluorescence-activated cell sorting (FACS)-purified GFP$^+$ cells obtained from E12.5 and E13.5 *Pitx3-GFP* embryos (Figure 3C), confirming their expression in mDA neurons *in vivo*. Hence, we investigated whether miR-34b/c and miR-148a-3p could act as post-transcriptional regulators of *Wnt1*. To this purpose we performed luciferase assays by transfecting plasmids expressing both miRNAs with a pmiR-reporter containing *Wnt1 3′UTR* in HeLa cells. Both miR-34b/c and miR-148a-3p were able to significantly reduce luciferase activity (34.6% and 20%, respectively). The effect was abolished after mutation of the predicted binding site for miR-34b/c but not for miR-148a-3p, suggesting that only miR-34b/c effectively binds to its predicted site at *Wnt1 3′UTR* (Figures 3B and 3D).

To further confirm that miR-34b/c and the Wnt signaling pathway could be involved in early phases of mDA differentiation, we used a dual-fluorescent GFP-reporter/monomeric red fluorescent protein (mRFP)-sensor plasmid (De Pietri Tonelli et al., 2006), which allows the detection of miRNAs at single-cell resolution. We cloned a tandem cassette complementary to miR-34b/c in the 3′ UTR of the mRFP sensor (pDSV3-34) or mutated in the region corresponding to the "seed sequence" of miR-34b/c (pDSV3-34mut). This approach has been described as very efficient for monitoring the endogenous expression of miRNAs both *in vitro* and *in vivo*. In differentiating mESCs transfected with pDSV3-34, the expression of the mRFP sensor was strongly reduced 72 hr after transfection (left column in Figure 3E). This effect was abolished with pDSV3-34mut (Figure 3E), thus suggesting that miR-34b/c is expressed *in vitro* during the DA differentiation of mESCs. Transfection of mESCs with the empty plasmids (pDSV2 and pDSV3) does not affect GFP or mRFP-sensor expression (Figure S1).

The endogenous miR-34b/c was also able to downregulate the expression of the mRFP sensor containing the entire *Wnt1 3′UTR* sequence downstream of the coding sequence (CDS) (pDSV2-UTR). A reduction for the mRFP sensor was clearly visible in mESCs transfected with pDSV2-UTR 72 hr after transfection (second right column in Figure 3E). Mutation in the binding site for miR-34b/c (pDSV2-UTRmut) did not affect the mRFP-sensor expression (right column in Figure 3E).

## Mir-34b/c Enhances mESC Dopaminergic Differentiation

Our data suggest that miR-34b/c has a role in DA neuron differentiation. To further corroborate this finding, we cloned ~900-bp genomic DNA encompassing the miR-34b/c cluster into an inducible lentiviral vector upstream of an Ires-GFP sequence (lenti-miR34b/c-Ires-GFP) and overexpressed the miR-34b/c cluster during the *in vitro* DA differentiation of mESCs. mESCs were infected with the lenti-miR34b/c-Ires-GFP vector (or with an inducible lenti-GFP as control), treated with doxycycline for 1 day and FACS purified for GFP. GFP$^+$ mESCs were amplified in the absence of doxycycline and then differentiated toward the DA phenotype in the presence or absence of doxycycline for 14 days (see scheme in Figure 4A). At the end of the differentiation, the expression of miR-34c was enriched 16-fold (Figure 4B), while no difference was observed for miR-34c in mock-infected GFP$^+$ mESCs (Figure 4B).

The overexpression of miR-34b/c cluster induced a downregulation in the mRNA levels for both *Wnt1* and *Lmx1b* (Figure 4C). Consistent with the RNA data, immunostaining revealed a significant reduction of LMX1B$^+$ cells (Figure S2). In parallel, we observed a reduced amount of mRNAs for *Lef1* and *Axin2*, thus supporting a role of miR-34b/c as a negative regulator of the Wnt signaling (Figure 4C). The overexpression of miR-34b/c also promoted DA differentiation. Indeed, we found a significant upregulation of mDA markers such as *Th*, *Dat*, *Vmat2*, and *Pitx3* (Figure 4D). In addition, miR34b/c overexpression resulted in a ~60% increase in the number of TH$^+$ cells compared with control cultures (Figures 4E and 4F).

## Mir-34b/c Enhances Fibroblast Transdifferentiation into Induced Dopaminergic Neurons

It has been shown that direct reprogramming represents a powerful source of iDA, useful for functional studies and cell replacement approaches. Hence, we further investigated whether miR-34b/c could increase the yield of DA neurons in such an experimental paradigm. To this purpose, we infected MEFs derived from mice expressing GFP under the control of the *Th* promoter (Sawamoto et al., 2001) with inducible lentiviruses expressing miR-34b/c cluster in combination with the reprogramming transcription factors *Ascl1* and *Nurr1* (renamed also A and N) (Caiazzo et al., 2011).

(D) Hierarchical clustering of mRNA in day 9 MD and day 14 MD of dopaminergic differentiation (+SHH/FGF8) and control (−SHH/FGF8). The cluster was built according to the expression profiles of differentially expressed genes of Wnt signaling pathway. The key color bar indicates that the expression levels increased from red to green. Boxes highlight the most significant differences. The most representative genes of Wnt pathway are reported on the right of the heatmap.
(E) The cartoon shows the most important genes involved in the Wnt pathway. Gray arrows indicate genes trend from array data.

Please cite this article in press as: De Gregorio et al., miR-34b/c Regulates *Wnt1* and Enhances Mesencephalic Dopaminergic Neuron Differentiation, Stem Cell Reports (2018), https://doi.org/10.1016/j.stemcr.2018.02.006

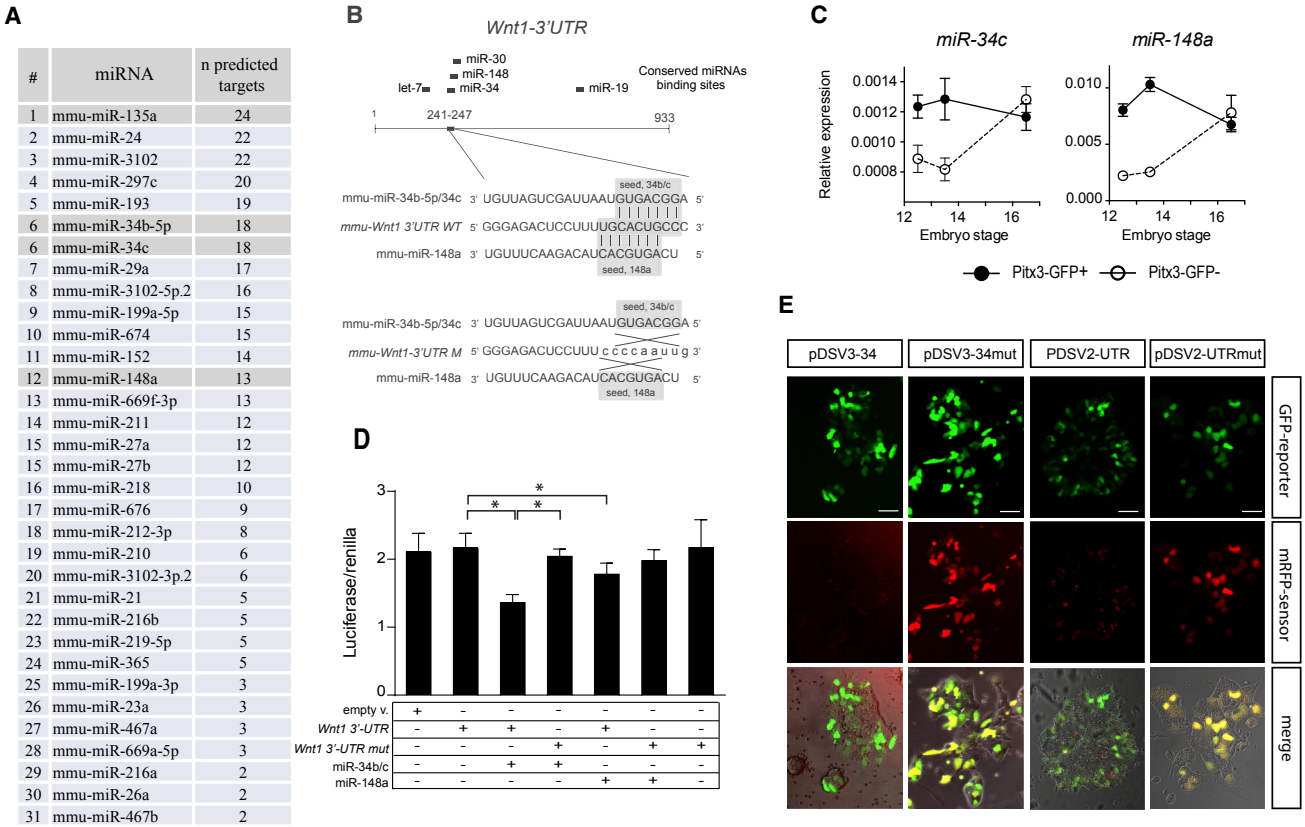


| # | miRNA | n predicted targets |
|---|---|---|
| 1 | mmu-miR-135a | 24 |
| 2 | mmu-miR-24 | 22 |
| 3 | mmu-miR-3102 | 22 |
| 4 | mmu-miR-297c | 20 |
| 5 | mmu-miR-193 | 19 |
| 6 | mmu-miR-34b-5p | 18 |
| 6 | mmu-miR-34c | 18 |
| 7 | mmu-miR-29a | 17 |
| 8 | mmu-miR-3102-5p.2 | 16 |
| 9 | mmu-miR-199a-5p | 15 |
| 10 | mmu-miR-674 | 15 |
| 11 | mmu-miR-152 | 14 |
| 12 | mmu-miR-148a | 13 |
| 13 | mmu-miR-669f-3p | 13 |
| 14 | mmu-miR-211 | 12 |
| 15 | mmu-miR-27a | 12 |
| 15 | mmu-miR-27b | 12 |
| 16 | mmu-miR-218 | 10 |
| 17 | mmu-miR-676 | 9 |
| 18 | mmu-miR-212-3p | 8 |
| 19 | mmu-miR-210 | 6 |
| 20 | mmu-miR-3102-3p.2 | 6 |
| 21 | mmu-miR-21 | 5 |
| 22 | mmu-miR-216b | 5 |
| 23 | mmu-miR-219-5p | 5 |
| 24 | mmu-miR-365 | 5 |
| 25 | mmu-miR-199a-3p | 3 |
| 26 | mmu-miR-23a | 3 |
| 27 | mmu-miR-467a | 3 |
| 28 | mmu-miR-669a-5p | 3 |
| 29 | mmu-miR-216a | 2 |
| 30 | mmu-miR-26a | 2 |
| 31 | mmu-miR-467b | 2 |

**Figure 3. miR-34b/c Targets *Wnt1* and Is Expressed in DA Neurons**

(A) Upregulated miRNAs obtained by comparing dopaminergic (+SHH/FGF8) with control protocols (−SHH/FGF8) both at day 9 MD and day 14 MD. For each miRNA, the number of predicted targets identified among the downregulated Wnt signaling genes is reported according to TargetScan algorithm. miRNAs selected for further investigation and miR-135a2 are highlighted.

(B) Schematic of the *Wnt1 3′UTR* reporting conserved miRNAs binding sites. The wild-type (3UTR WT) and mutated (3UTR M) seed sequences for miR-34b/c and miR-148a-3p are highlighted.

(C) TaqMan assay for the expression of miR-34c and miR-148a-3p in FACS-purified PITX3-GFP$^+$ and PITX3-GFP$^-$ cells at E12.5, E13.5, and E16.5. Data are normalized to the average of the reference sno-202 and represent mean ± SEM of three independent experiments.

(D) Luciferase assay. pmiR-Reports containing the wild-type (*Wnt1 3′UTR*) or mutated (*Wnt1 3′UTRmut*) 3′ untranslated sequence for *Wnt1* were co-transfected with Tet-O-FUW-miR-34b/c plus rtTA (miR-34b/c) and Tet-O-FUW-miR-148a-3p plus rtTA (miR-148a). The empty pmiR-Report vector was used as additional control. All luciferase data have been normalized to the Renilla (RL-SV40) activity. Data represent mean ± SEM from three independent experiments. *$p < 0.01$ (Student's t test).

(E) Dual-fluorescent reporter assay based on GFP reporter and monomeric red fluorescent protein sensor (mRFP). Left columns: ESCs transfected with; a plasmid containing a complementary sequence to miR-34b/c downstream the CDS for the mRFP sensor (pDSV3-34) or, with a plasmid containing a sequence mutated in the region corresponding to the "seed" for miR-34b/c (pDSV3-34mut). Right columns: ESCs transfected with a plasmid containing the wild-type *Wnt1 3′UTR* (pDSV2-UTR) or mutated in the binding site for miR-34b/c (pDSV3-UTRmut) downstream of the CDS for the mRFP sensor. Images were acquired 72 hr after transfection. Scale bars, 50 μm.

The expression of miR-34b/c in combination with *Ascl1* and *Nurr1* was induced 1 day after the infection by adding doxycycline to the culture medium. Cells were then differentiated for 14 days (day 14 MD) before analyzing the amount of TH$^+$ and GFP$^+$ cells. FACS analysis revealed that the combination of miR-34b/c with ASCL1 and NURR1 (AN versus AN + 34b/c) increased the number of GFP$^+$ cells from 10.1% ± 1.7% to 19.5% ± 2.4% (Figures 5A and 5B) while miR-34b/c alone or in combination with ASCL1 was unable to induce GFP expression (our unpublished data). Such a difference was further verified by an increased level of *Th* mRNA (Figure 5H) and the number of TH$^+$ cells following quantification of captured images (Figures 5C and 5E).

The addition of miR-34b/c affects terminal differentiation of DA neurons. Indeed, the expression of late mDA-specific markers such as *Dat* and *Vmat2* were increased at mRNA level when miR-34b/c was combined with ASCL1 and NURR1 (AN34 versus AN in Figures 5I and 5J).

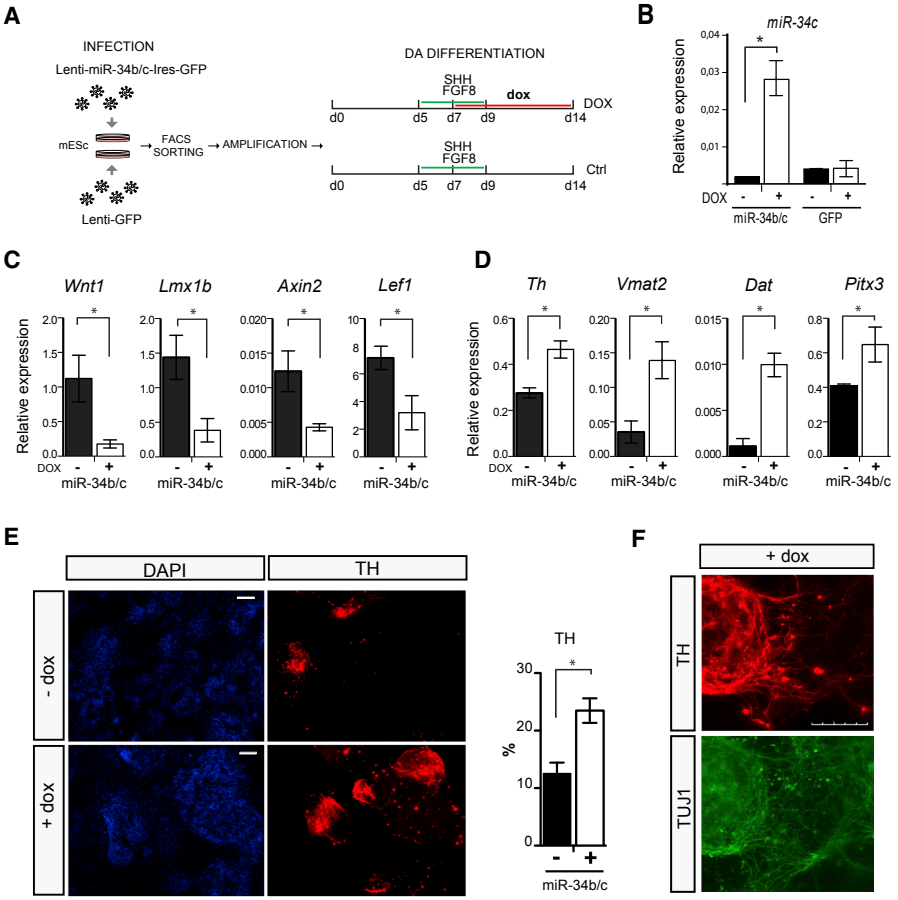


**Figure 4. Enforced Expression of miR-34b/c Promotes ESC DA Differentiation by Downregulating Wnt Signaling**

(A) Schematic representation of the experimental procedure. mESCs were infected with an inducible lentiviral vector expressing miR-34b/c upstream of an Ires-GFP sequence. Cells were FACS purified, amplified, and differentiated toward the DA phenotype.

(B) TaqMan assay for miR-34c in FACS purified mESCs in presence or absence of doxycycline (DOX). Data were normalized to the average of the reference sno-202. Data represent mean ± SEM. *$p < 0.01$ (Student's t test).

(C and D) qPCR analysis of genes related to the Wnt pathway (*Wnt1*, *Lmx1b*, *Axin2*, and *Lef1*; C) and dopaminergic lineage (*Th*, *Vmat2*, *Dat*, and *Pitx3*; D) at day 14 MD in the presence or absence of DOX. Data represent mean ± SEM from three independent experiments. *$p < 0.01$ (Student's t test).

(E and F) Immunostaining and quantifications for TH in mESCs at day 14 MD (E). Counting was performed from 20 randomly selected fields for each condition, in three independent experiments. Data represent mean ± SEM. *$p < 0.05$ relative to −DOX (Student's t test). A higher-magnification image of DA-differentiated ESCs is shown in (F). TH (red) and TUBB3 (green). Scale bars represent 200 μm in (E) and 100 μm in (F).

To understand whether miR-34b/c acts by affecting cell cycle progression, we infected the neuronal cell line A1 (Colucci-D'Amato et al., 1999) with an inducible lenti-miR34b/c-Ires-GFP (lenti-miR34b/c-Ires-GFP) or a control lenti-GFP virus and analyzed FACS-purified $GFP^+$ cells by quantitating of DNA content. Forty-eight hours after infection, we observed that cultures infected with miR-34b/c (lenti-miR34b/c) contained more cells in $G_0/G_1$ (74.5% ± 3%) than those in control culture (61% ± 1%, Figures S3A and S3B).

To investigate whether the modulation of Wnt signaling may have a role in the transdifferentiation process, we infected MEFs derived from TH-GFP mice with *Ascl1*, *Nurr1*, and miR-34b/c in the presence of CHIR99021 (chiron), a selective inhibitor of GSK3β that can mimic Wnt activation. We found that while chiron did not alter the level of *Wnt1* (AN34C in Figure 5F), it elicited a strong upregulation of *Lef1* (AN34C in Figure 5G), suggesting an activation of Wnt signaling as expected. This effect was accompanied by a significant reduction in both the number of $TH^+$ neurons (AN34C in Figures 5C, 5D, and 5H) and the transcript level of several mDA markers such as *Vmat2* and *Dat* (AN34C in Figures 5H and 5J).

Please cite this article in press as: De Gregorio et al., miR-34b/c Regulates *Wnt1* and Enhances Mesencephalic Dopaminergic Neuron Differentiation, Stem Cell Reports (2018), https://doi.org/10.1016/j.stemcr.2018.02.006

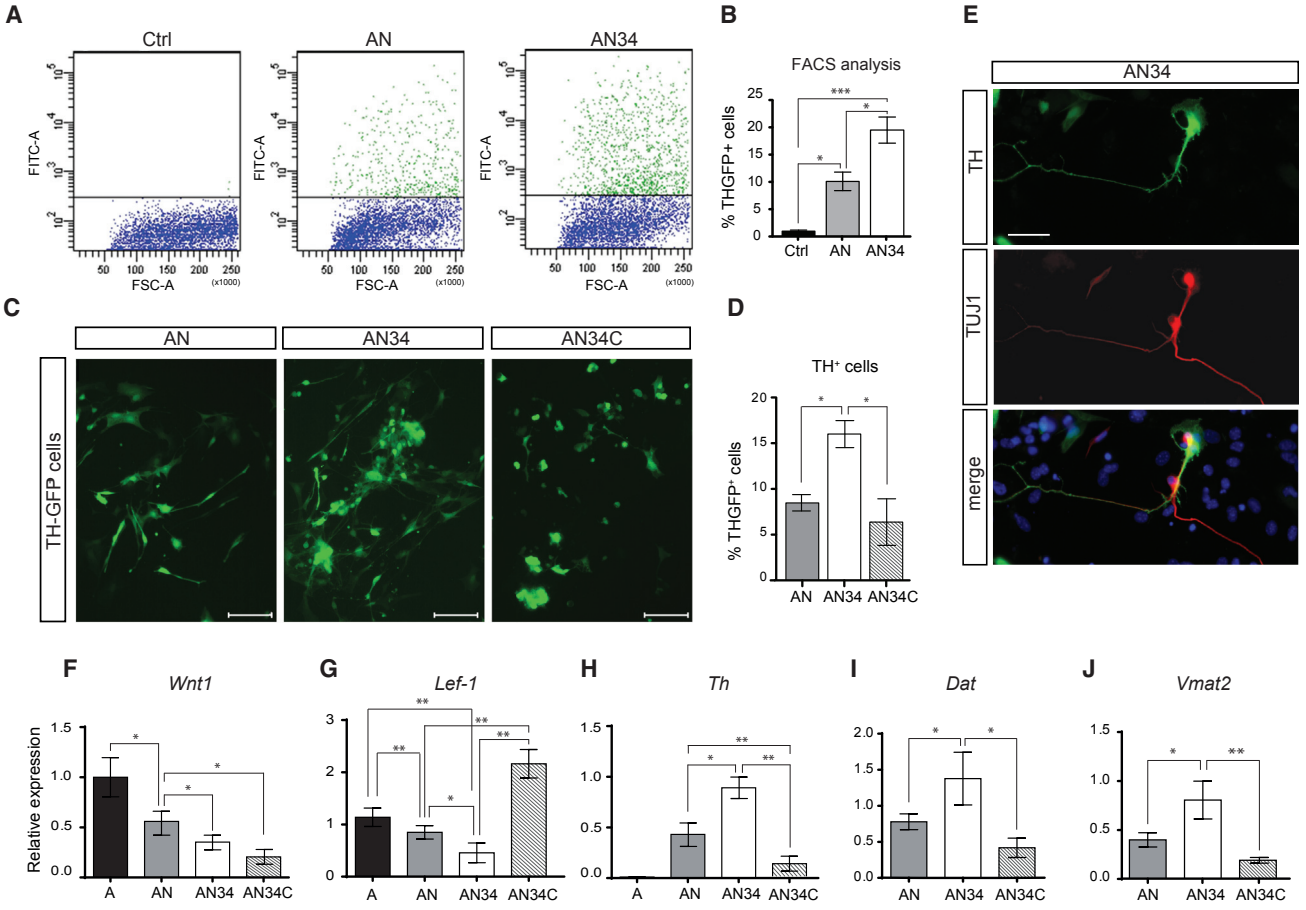


**Figure 5. miR-34b/c Enhances Dopaminergic Transdifferentiation**

(A and B) MEFs, derived from TH-GFP mice, transdifferentiated into DA neurons (iDA) with; ASCL1 and NURR1 (AN) or; ASCL1, NURR1 and miR-34b/c (AN34) and analysed by FACS (A). The percentage of TH-GFP$^+$ cells is shown in (B).

(C–E) Representative pictures of iDA obtained with AN, AN34, or AN34 plus CHIR99021 (AN34C), a potent activator of the Wnt pathway (C), and relative quantification (D). Scale bar represents 100 μm. (E) A representative image of iDA neurons obtained with AN34; TH is in green and TUBB3 in red. Scale bar represents 25 μm.

(F and G) qPCR for *Wnt1* (F) and its downstream target *Lef1* (G) of MEFs transdifferentiated with ASCL1 alone (A), ASCL1 and NURR1 (AN), or ASCL1, NURR1, and miR-34b/c in the presence or absence of chiron (AN34 or AN34C).

(H–J) qPCR for the expression of dopaminergic genes *Th* (H), *Dat* (I), and *Vmat2* (J) in iDA obtained with AN, AN34, or AN34C. qPCR data for gene expression have been normalized to the average of the reference gene *Hmbs*.

Data represent mean ± SEM from three independent experiments. *p < 0.05; **p < 0.01; ***p < 0.001 (Newman-Keuls test).

## Mir-34b/c Programmed iDA Cells Are Functionally Active

MEF-derived iDA by miR-34b/c direct reprogramming also contains higher amounts of dopamine, as shown after staining with an anti-DA antibody (Figures 6A and 6B). Higher amounts of double-positive (DA$^+$, TH-GFP$^+$) cells (16.1% ± 2.3% versus 6.9% ± 2.5%) were identified when miR-34b/c was included in the reprogramming cocktail (AN34 versus AN) (Figure 6B). Similarly, a higher content of dopamine was also shown by high-performance liquid chromatography (HPLC) measurements (Figure 6C), suggesting an increased dopamine synthesis in miR34-b/c-derived iDA.

To directly demonstrate that miR-34b/c-derived iDA are functional, we measured the action potential by performing targeted whole-cell electrophysiological recordings. TH-GFP$^+$ cells derived from miR-34b/c displayed active neuronal properties. In extracellular recordings, we recorded spontaneous action potential firing at 3.93 ± 2.28 Hz in four cells. These events were reversibly blocked by TTX (1 μM), suggesting that they were mainly mediated by sodium currents (Figure 6D). In whole-cell recordings, depolarizing current injection of increasing amplitudes from a holding potential of −55/−60 mV (1 s, Figure 6E) evoked trains of action potentials in five cells, which were

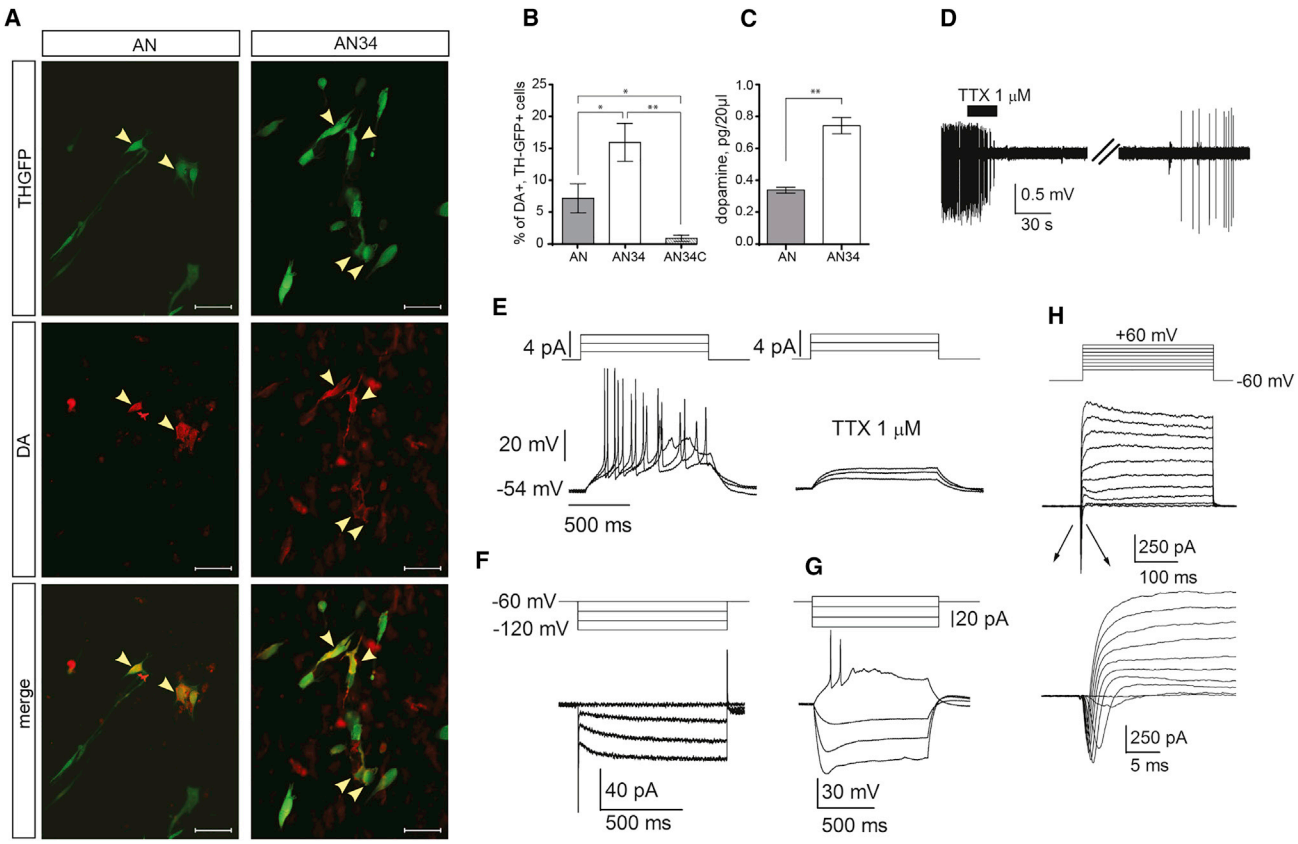


**Figure 6. miR-34b/c-Derived iDA Cells Are Functionally Active**

(A and B) MEFs derived from TH-GFP mice were transdifferentiated in the presence of AN or AN34 and immunostained with and anti-DA antibody. Arrowheads indicate double-positive ($DA^+$; $TH\text{-}GFP^+$) cells. Scale bar represents 50 µm. Quantification of $DA^+$; $TH\text{-}GFP^+$ cells is shown in (B). Data represent mean ± SEM from three independent experiments. *$p < 0.05$; **$p < 0.01$ (Newman-Keuls test).

(C) HPLC analysis of dopamine content in AN- and AN34-derived iDA cells; Data represent mean ± SEM from three independent experiments; **$p < 0.01$ (Student's t test).

(D–H) Spontaneous firing activity of iDA neurons during extracellular single-unit recording is reversibly inhibited by TTX (D). In whole-cell recordings, injection of depolarizing current steps from a holding potential of −54 mV evoked trains of action potentials (E, left) that were blocked by TTX (E, right), suggesting that they are mediated by fast $Na^+$ currents. Hyperpolarization-activated membrane currents (F) and sag potentials (G) indicate the expression of $I_h$ in iDA neurons. Typical voltage-dependent inward and outward currents (H) are also present in iDA neurons.

completely blocked by TTX (Figure 6E, right), similar to those seen in *ex vivo* DA neurons. In response to the same protocol, another group of cells displayed membrane depolarization that did not reach the threshold for action potential generation (not shown).

In voltage-clamp recordings (Figure 6F, $V_h = -60$ mV), we applied hyperpolarizing voltage steps (to −120 mV, 20-mV increments) to activate the hyperpolarization-activated inward current, $I_h$, largely expressed *in vivo* by DA neurons of the *substantia nigra pars compacta* (Grace and Onn, 1989; Mercuri et al., 1995) and to a lesser extent by some neurons of the ventral tegmental area (Krashia et al., 2017) Two out of the 25 recorded $GFP^+$ cells displayed a small $I_h$ (Figure 6F) and a sag potential in response to hyperpolarizing current injections in current clamp mode (Figure 6G). Voltage-gated $Na^+$ and $K^+$ currents elicited by depolarizing voltage steps are also shown (Figure 6H). Taken together, these data confirm that miR-34b/c-derived iDA behave as functional active DA neurons.

## DISCUSSION

### Mir-34b/c Is Expressed in mDA Neurons and Regulates *Wnt1*

In the midbrain Wnt signaling is required for DA neurogenesis, and among the multiple canonical Wnts *Wnt1* and

*Wnt5a* have a well-established role in promoting DA differentiation (Arenas, 2014). Here we investigate whether miRNAs could have a role in DA neuron differentiation alongside the Wnt signaling genes, since it was shown recently that restriction of *Wnt1* and the downstream Wnt signaling occurs during mDA development and is achieved by a feedback loop including miR-135a2-5p that acts by repressing *Lmx1b*, and modulating WNT1/Wnt signaling (Anderegg et al., 2013). Interestingly we identified miR-135a2-5p as the miRNA with the highest number of predicted targets among the genes associated with Wnt pathway, which were downregulated at the late phases of our DA differentiation experiment (between day 9 and day 14 MD), confirming the relevance of our analysis aimed at identifying novel candidate miRNAs playing a role during DA differentiation. This approach allowed us to identify also miR-148a-3p and miR-34b/c, two miRNAs, enriched in FACS-purified mDA neurons, which are predicted to target *Wnt1 3′UTR*. Nevertheless only miR-34b/c binds the *Wnt1 3′UTR* and represses luciferase activity.

While the function of miR-34a in regulating Wnt signaling has been shown in both cancer progression and development (Kim et al., 2011, 2013), the involvement of miR-34b/c in this pathway has been largely neglected mainly because of the assumption that miRNAs sharing identical seed sequences target the same genes. It is now clear, however, that the role of individual miRNA should be considered relative to the cellular context and that sequence determinants outside the seed might profoundly affect miRNA binding through undefined mechanisms (Navarro and Lieberman, 2015; Ebner and Selbach, 2014).

Interestingly miR-34b/c was previously shown to be downregulated in postmortem brain of PD patients at different stages of pathology (Miñones-Moyano et al., 2011). Nevertheless, few papers described the involvement of miR-34b/c in mDA neurons or reported DA-related phenotypes in miR-34b/c knockout mice (Comazzetto et al., 2014; Concepcion et al., 2012). This may be explained by the redundancy between the miR-34 family that includes three members of miR-449 (a, b, and c) in addition to miR-34a, b, and c. It is plausible that *in vivo* fine-tuning of the Wnt signaling might require the action of several miRNAs targeting simultaneously different actors of the pathway. In this context, it is not surprising that deletion of a single gene cluster has limited or no effects on mDA development.

Thus, although we identify *Wnt1* as a target of miR-34b/c, it is unlikely that downregulation of *Wnt1* by itself could drive mDA differentiation. We believe, indeed, that the miR-34b/c-mediated downregulation of *Wnt1* is part of a complex series of events requiring the simultaneous intervention of other genes and pathways whose final aim is to define DA identity.

## Mir-34b/c Potentiates iDA Reprogramming

Direct reprogramming has been used to achieve differentiation of fibroblasts into specific subtypes of mature neurons (Vierbuchen et al., 2010) and is considered a promising approach in terms of both regenerative medicine and modeling human diseases. For DA neurons this result has been achieved by combinatorial expression of early and late mDA transcription factors such as *Ascl1*, *Lmx1a*, and *Nurr1* (Caiazzo et al., 2011). miRNAs are considered a very promising additional tool to increase the yield of specific neuronal populations, as was shown by miR-9 and miR-124 (Victor et al., 2014). A similar mechanism may be proposed also for miR-34b/c, which increases mDA differentiation efficiency by facilitating cell cycle exit through the upregulation of a potent cyclin-dependent kinase inhibitor *p21* (our unpublished data). The expression of miR-34b/c during the differentiation phases in combination with ASCL1 and NURR1 represses proliferation, promotes terminal differentiation, and downregulates *Wnt1*, which was maintained at high level by constant expression of *Ascl1* (Rheinbay et al., 2013). The importance of miR-34b/c has also emerged in previous reports that placed miR-34 downstream of *p53* (Kim et al., 2011). miRNAs might thus be required to shut down molecular programs to counteract differentiation. In DA neurons this is the case for miR-124 (Jiang et al., 2015) and miR-34b/c, which facilitate the generation of functional active DA neurons.

In the brain, miRNAs confer robustness to specific developmental processes and contribute to the maturation of specific neuronal circuits (Amin et al., 2015; Choi et al., 2008; Conaco et al., 2006; Cuellar et al., 2008; Tan et al., 2013, Stark et al., 2005). It is thus possible that miR-34b/c acts, at least in part, along the same axis by restraining Wnt signaling in the midbrain, thus facilitating cell cycle exit and allowing progenitor differentiation toward mature DA neurons. Taken together, our findings suggest that the achievement of functional mDA neurons requires the control over time of different stimuli (such as those mediated by the Wnt signaling) that are essential during early progenitor differentiation. It is plausible that other miRNAs are involved in the DA-differentiation process through the regulation of different pathways. It will be thus compelling to attain their identification in order to further understand the process of DA differentiation and increase the overall yield of DA neurons, as well as to improve their features in terms of both molecular and physiological properties.

Please cite this article in press as: De Gregorio et al., miR-34b/c Regulates *Wnt1* and Enhances Mesencephalic Dopaminergic Neuron Differentiation, Stem Cell Reports (2018), https://doi.org/10.1016/j.stemcr.2018.02.006

## EXPERIMENTAL PROCEDURES

### Ethics Statement

All procedures involving mice were carried out in strict accordance with national and European law.

### EpiSC DA Differentiation

Dopaminergic differentiation of epiSC was performed as previously described (Jaeger et al., 2011). The sequential steps of the protocol are described in the Supplemental Experimental Procedures.

### RNA Extraction and qPCR

RNA was extracted from cells and tissues using the TRI-Reagent (Sigma, Milan, Italy) or miRVana miRNA isolation kit (Ambion, Milan, Italy). qPCR was carried out at least in triplicate samples using Power SYBR Green or TaqMan microRNA assays (Applied Biosystems, Milan, Italy) and analyzed as described in Supplemental Experimental Procedures.

### Microarray Data Analysis

Microarray data were performed on epiSC differentiated toward the DA phenotype as described in Supplemental Experimental Procedures. Data are available at GEO: GSE110270.

Gene ontology and pathway analysis were performed on microarray data using the DAVID functional annotation tool (https://david.ncifcrf.gov) (Huang et al., 2007b) to find over-represented biological themes. Default DAVID parameters were used. To identify the pathways altered, we used the online tool available from Kanehisa laboratories, KEGG Mapper (Kanehisa et al., 2010). Regarding putative miRNA-mRNA interaction, for the identification of miRNA responsive elements within the 3′ UTRs of protein coding genes, we used TargetScan algorithm (Lewis et al., 2005).

### PITX3-GFP$^+$ Cell Analysis

Freshly dissected ventral midbrains of *Pitx3-GFP* embryos were dissociated using a Papain dissociation system (Worthington, Milan, Italy). GFP-positive and -negative cells were isolated by a Cytopeia Influx Cell sorter or BD FACSAria III using previously described settings (Jacobs et al., 2011) and collected in RNAlater (Thermo Fisher Scientific, Milan, Italy). RNA was then purified by an miRVana miRNA isolation kit and analyzed by TaqMan MicroRNA Assays as described in Supplemental Experimental Procedures.

### Immunocytochemistry

The following primary antibodies were used with the protocol described in Supplemental Experimental Procedures: anti-TUJ1 mouse 1:1,000 (Covance, Rome, Italy, catalog #MMS-435P), anti-TH rabbit 1:500 (Chemicon, Milan, Italy, cat. #AB152), anti-LMX1B rabbit (a gift from Dr. Antonio Simeone), and anti-GFP mouse (Thermo Fisher Scientific, cat. #A11120). Dopamine staining was performed with an anti-dopamine rabbit (IS1005) + STAINperfect immunostaining kit A (SP-A-1000) (ImmuSmol SAS, Bordeaux, France) according to the manufacturer's instruction.

### Image Quantification

Images were acquired using a Leica TCS SP5 confocal microscope. Quantification was performed either by using the cell counter plugin in the ImageJ software on randomly selected fields or by performing pixel analysis quantifications with a custom-made ImageJ plugin (rsb.info.nih.gov/ij/download/). In both cases quantification was performed from at least three independent experiments.

### Luciferase Assay

The assay was performed by using the Luciferase Reporter Assay System (Promega, Milan, Italy), following the manufacturer's instructions. The 3′ UTR-containing pmiR-Report was co-transfected with the Tet-O-FUW miRNA-overexpressing vector and the rtTA-expressing vector in HeLa cells. A pRL-SV40 Renilla luciferase reporter vector (Promega) was also used to quantify the transfection efficiency. Firefly luciferase luminescent signal was normalized on the Renilla luciferase signal. For each assay, a control experiment with the empty pmiR-Report vector or without overexpressing any miRNA were performed.

### Dual-Fluorescent Reporter Sensor

DFRS plasmids were kindly provided by Prof. Wieland B. Huttner. Cloning strategy was performed as previously described (De Pietri Tonelli et al., 2014) using the oligos listed in Supplemental Experimental Procedures. Plasmids were transfected into control (basal) and differentiating mESCs by Lipofectamine. Fluorescence was monitored every day until 72 hr post transfection.

### Lentivirus Preparation and Viral Infection

cDNAs for *mAscl1*, *mNurr1*, and 983 base pairs encompassing the pri-miRNA-34b/c cluster were cloned into Tet-O-FUW or Tet-O-FUW-Ires-GFP lentiviral vectors under the control of the tetracycline operator. Lentiviruses were packaged in HEK293T cells as previously described (Caiazzo et al., 2011) (see Supplemental Experimental Procedures for details). Gene expression was tested by qPCR, while miRNA levels were measured by TaqMan assay. Infections were performed in combination of rtTA transactivator viruses supplied with doxycycline (2 μg/mL, Clontech).

### Fluorescence-Activated Cell Sorting

TH-GFP$^+$ iDA cells or mES-miR-34b/c-GFP$^+$ cells were trypsinized, washed, and sorted or analyzed with a BD FACSAria II. Cells were collected in TRI-Reagent (Sigma) for RNA extraction or in cell culture medium for subsequent amplification.

### Induced Dopaminergic Neuron Generation

iDA neurons were generated from MEFs as previously described (Caiazzo et al., 2011). In brief, MEFs were infected with rtTA, Tet-O-FUW-*mAscl1*, Tet-O-FUW-*mNurr1*, and Tet-O-FUW-miR-34b/c lentiviruses in MEF medium with addition of doxycycline (2 μg/mL, Sigma). After 48 hr the medium was replaced with neuronal inducing medium (DMEM/F12, B27, and penicillin/streptomycin [all from Thermo Fisher Scientific]) containing doxycycline and cells cultured for 14 days.

### Electrophysiology Recordings

Whole-cell patch-clamp and conventional single-unit extracellular recordings were performed according to published procedures (Guatteo et al., 2013, 2017) from visually identified TH-GFP$^+$ cells plated on glass coverslips at 12–16 days post infection. See Supplemental Experimental Procedures for details.

### Statistical Analysis

All statistical analyses were performed using GraphPad Prism (GraphPad Software). Significance of differences was assessed by one-way ANOVA followed by Newman-Keuls post hoc test for intergroup comparisons or by Student's t test when cultures were compared with the corresponding control or with vehicle.

## ACCESSION NUMBERS

The accession number for microarray data reported in this paper is GEO: GSE110270.

## SUPPLEMENTAL INFORMATION

Supplemental Information includes Supplemental Experimental Procedures, three figures, and one table and can be found with this article online at https://doi.org/10.1016/j.stemcr.2018.02.006.

## AUTHOR CONTRIBUTIONS

Conceived and designed the experiments: G.C.B., R.D.G., S.P., V.C., M.L., N.B.M., and E.G. Performed screening, initial characterization, and ESC differentiation: R.D.G. Performed transdifferentiation experiments and mRFP-sensor analysis: S.P. and C.D.S. Performed luciferase assay: C.D.S. and R.D.G. Performed electrophysiology: E.G., R.M.P., and N.B.M. Contributed reagents/materials/analysis tools: S.P., R.D.G., M.S., R.E., C.D.S., F.V., V.C., L.v.O., M.C., D.G., R.M.P., E.C.L., and S.P.-A. Analyzed the data: G.C.B., R.G.D., S.P., C.P.C., U.d.P., E.G., and N.B.M. Wrote the paper: G.C.B., R.D.G., S.P., E.G., and M.L.

## ACKNOWLEDGMENTS

We thank FIRB-RBIN062YH4, MERIT-RBNE08LN4P-002, PRIN 2015R9ASHT_003, and Finanziamento Ricerca di Ateneo to C.P.C. for financial support. We also thank Sara Mancinelli who provided the Tet-O-FUW-Ires-GFP empty vector and Dr. Antonio Simeone for anti-LMX1B antibody. We are grateful to the FACS facility and the Integrated Microscopy Facility of the Institute of Genetics and Biophysics "Adriano Buzzati Traverso," CNR, Naples, Italy.

Received: April 24, 2017
Revised: February 9, 2018
Accepted: February 9, 2018
Published: March 8, 2018

## REFERENCES

Agarwal, V., Bell, G.W., Nam, J.W., and Bartel, D.P. (2015). Predicting effective microRNA target sites in mammalian mRNAs. Elife *4*. https://doi.org/10.7554/eLife.05005, e05005.

Amin, N.D., Bai, G., Klug, J.R., Bonanomi, D., Pankratz, M.T., Gifford, W.D., Hinckley, C.A., Sternfeld, M.J., Driscoll, S.P., Dominguez, B., et al. (2015). Loss of motoneuron-specific microRNA-218 causes systemic neuromuscular failure. Science *350*, 1525–1529.

Anderegg, A., Lin, H.P., Chen, J.A., Caronia-Brown, G., Cherepanova, N., Yun, B., Joksimovic, M., Rock, J., Harfe, B.D., Johnson, R., et al. (2013). An lmx1b-miR135a2 regulatory circuit modulates Wnt1/wnt signaling and determines the size of the midbrain dopaminergic progenitor pool. PLoS Genet. *9*, e1003973.

Arenas, E. (2014). Wnt signaling in midbrain dopaminergic neuron development and regenerative medicine for Parkinson's disease. J. Mol. Cell Biol. *6*, 42–53.

Bartel, D.P., and Chen, C.Z. (2004). Micromanagers of gene expression: the potentially widespread influence of metazoan microRNAs. Nat. Rev. Genet. *5*, 396–400.

Caiazzo, M., Dell'Anno, M.T., Dvoretskova, E., Lazarevic, D., Taverna, S., Leo, D., Sotnikova, T.D., Menegon, A., Roncaglia, P., Colciago, G., et al. (2011). Direct generation of functional dopaminergic neurons from mouse and human fibroblasts. Nature *477*, 224–227.

Choi, P.S., Zakhary, L., Choi, W.Y., Caron, S., Alvarez-Saavedra, E., Miska, E.A., McManus, M., Harfe, B., Giraldez, A.J., Horvitz, H.R., et al. (2008). Members of the miRNA-200 family regulate olfactory neurogenesis. Neuron *57*, 41–55.

Colucci-D'Amato, G.L., Tino, A., Pernas-Alonso, R., ffrench-Mullen, J.M., and di Porzio, U. (1999). Neuronal and glial properties coexist in a novel mouse CNS immortalized cell line. Exp. Cell Res. *1*, 383–391.

Comazzetto, S., Di Giacomo, M., Rasmussen, K.D., Much, C., Azzi, C., Perlas, E., Morgan, M., and O'Carroll, D. (2014). Oligoasthenoteratozoospermia and infertility in mice deficient for miR-34b/c and miR-449 loci. PLoS Genet. *10*, e1004597.

Conaco, C., Otto, S., Han, J.J., and Mandel, G. (2006). Reciprocal actions of REST and a microRNA promote neuronal identity. Proc. Natl. Acad. Sci. USA *103*, 2422–2427.

Concepcion, C.P., Han, Y.C., Mu, P., Bonetti, C., Yao, E., D'Andrea, A., Vidigal, J.A., Maughan, W.P., Ogrodowski, P., and Ventura, A. (2012). Intact p53-dependent responses in miR-34-deficient mice. PLoS Genet. *8*, e1002797.

Cuellar, T.L., Davis, T.H., Nelson, P.T., Loeb, G.B., Harfe, B.D., Ullian, E., and McManus, M.T. (2008). Dicer loss in striatal neurons produces behavioral and neuroanatomical phenotypes in the absence of neurodegeneration. Proc. Natl. Acad. Sci. USA *105*, 5614–5619.

Davis, T.H., Cuellar, T.L., Koch, S.M., Barker, A.J., Harfe, B.D., McManus, M.T., and Ullian, E.M. (2008). Conditional loss of Dicer disrupts cellular and tissue morphogenesis in the cortex and hippocampus. J. Neurosci. *28*, 4322–4330.

De Pietri Tonelli, D., Calegari, F., Fei, J.F., Nomura, T., Osumi, N., Heisenberg, C.P., and Huttner, W.B. (2006). Single-cell detection of microRNAs in developing vertebrate embryos after acute administration of a dual-fluorescence reporter/sensor plasmid. Biotechniques *41*, 727–732.

De Pietri Tonelli, D., Clovis, Y.M., and Huttner, W.B. (2014). Detection and monitoring of microRNA expression in developing mouse brain and fixed brain cryosections. Methods Mol. Biol. *1092*, 31–42.

Ebner, O.A., and Selbach, M. (2014). Quantitative proteomic analysis of gene regulation by miR-34a and miR-34c. PLoS One *9*, e92166.

Gennet, N., Gale, E., Nan, X., Farley, E., Takacs, K., Oberwallner, B., Chambers, D., and Li, M. (2011). Doublesex and mab-3-related transcription factor 5 promotes midbrain dopaminergic identity in pluripotent stem cells by enforcing a ventral-medial progenitor fate. Proc. Natl. Acad. Sci. USA *108*, 9131–9136.

Grace, A.A., and Onn, S.P. (1989). Morphology and electrophysiological properties of immunocytochemically identified rat dopamine neurons recorded in vitro. J. Neurosci. *9*, 3463–3481.

Guatteo, E., Yee, A., McKearney, J., Cucchiaroni, M.L., Armogida, M., Berretta, N., Mercuri, N.B., and Lipski, J. (2013). Dual effects of L-DOPA on nigral dopaminergic neurons. Exp. Neurol. *247*, 582–594.

Guatteo, E., Rizzo, F.R., Federici, M., Cordella, A., Ledonne, A., Latini, L., Nobili, A., Viscomi, M.T., Biamonte, F., Landrock, K.K., et al. (2017). Functional alterations of the dopaminergic and glutamatergic systems in spontaneous α-synuclein overexpressing rats. Exp. Neurol. *287*, 21–33.

Guo, C., Qiu, H.Y., Huang, Y., Chen, H., Yang, R.Q., Chen, S.D., Johnson, R.L., Chen, Z.F., and Ding, Y.Q. (2007). Lmx1b is essential for Fgf8 and Wnt1 expression in the isthmic organizer during tectum and cerebellum development in mice. Development *134*, 317–325.

Huang, D.W., Sherman, B.T., Tan, Q., Collins, J.R., Alvord, W.G., Roayaei, J., Stephens, R., Baseler, M.W., Lane, H.C., and Lempicki, R.A. (2007a). The DAVID Gene Functional Classification Tool: a novel biological module-centric algorithm to functionally analyze large gene lists. Genome Biol. *8*, R183.

Huang, D.W., Sherman, B.T., Tan, Q., Kir, J., Liu, D., Bryant, D., Guo, Y., Stephens, R., Baseler, M.W., Lane, H.C., et al. (2007b). DAVID Bioinformatics Resources: expanded annotation database and novel algorithms to better extract biology from large gene lists. Nucleic Acids Res. *35*, W169–W175.

Jacobs, F.M., Veenvliet, J.V., Almirza, W.H., Hoekstra, E.J., von Oerthel, L., van der Linden, A.J., Neijts, R., Koerkamp, M.G., van Leenen, D., Holstege, F.C., et al. (2011). Retinoic acid-dependent and -independent gene-regulatory pathways of Pitx3 in mesodiencephalic dopaminergic neurons. Development *138*, 5213–5222.

Jaeger, I., Arber, C., Risner-Janiczek, J.R., Kuechler, J., Pritzsche, D., Chen, I.C., Naveenan, T., Ungless, M.A., and Li, M. (2011). Temporally controlled modulation of FGF/ERK signaling directs midbrain dopaminergic neural progenitor fate in mouse and human pluripotent stem cells. Development *138*, 4363–4374.

Jiang, H., Xu, Z., Zhong, P., Ren, Y., Liang, G., Schilling, H.A., Hu, Z., Zhang, Y., Wang, X., Chen, S., Yan, Z., and Feng, J. (2015). Cell cycle and p53 gate the direct conversion of human fibroblasts to dopaminergic neurons. Nat. Commun. *6*, 10100.

Joksimovic, M., and Awatramani, R. (2014). Wnt/ß-catenin signaling in midbrain dopaminergic neuron specification and neurogenesis. J. Mol. Cell Biol. *6*, 27–33.

Judson, R.L., Babiarz, J.E., Venere, M., and Blelloch, R. (2009). Embryonic stem cell-specific microRNAs promote induced pluripotency. Nat. Biotech. *27*, 459–461.

Kanehisa, M., Goto, S., Furumichi, M., Tanabe, M., and Hirakawa, M. (2010). KEGG for representation and analysis of molecular networks involving diseases and drugs. Nucleic Acids Res. *38*, D355–D360.

Kapsimali, M., Kloosterman, W.P., de Bruijn, E., Rosa, F., Plasterk, R.H., and Wilson, S.W. (2007). MicroRNAs show a wide diversity of expression profiles in the developing and mature central nervous system. Genome Biol. *8*, R173.

Kawase-Koga, Y., Otaegi, G., and Sun, T. (2009). Different timings of Dicer deletion affect neurogenesis and gliogenesis in the developing mouse central nervous system. Dev. Dyn. *238*, 2800–2812.

Kim, J., Inoue, K., Ishii, J., Vanti, W.B., Voronov, S.V., Murchison, E., Hannon, G., and Abeliovich, A. (2007). A MicroRNA feedback circuit in midbrain dopamine neurons. Science *317*, 1220–1224.

Kim, N.H., Cha, Y.H., Kang, S.E., Lee, Y., Lee, I., Cha, S.Y., Ryu, J.K., Na, J.M., Park, C., Yoon, H.G., et al. (2013). p53 regulates nuclear GSK-3 levels through miR-34-mediated Axin2 suppression in colorectal cancer cells. Cell Cycle *12*, 1578–1587.

Kim, N.H., Kim, H.S., Kim, N.G., Lee, I., Choi, H.S., Li, X.-Y., Kang, S.E., Cha, S.Y., Ryu, J.K., Na, J.M., et al. (2011). p53 and microRNA-34 are suppressors of canonical Wnt signaling. Sci. Signal. *4*, ra71.

Krashia, P., Martini, A., Nobili, A., Aversa, D., D'Amelio, M., Berretta, N., Guatteo, E., and Mercuri, N.B. (2017). On the properties of identified dopaminergic neurons in the mouse substantia nigra and ventral tegmental area. Eur. J. Neurosci. *45*, 92–105.

Lewis, B.P., Burge, C.B., and Bartel, D.P. (2005). Conserved seed pairing, often flanked by adenosines, indicates that thousands of human genes are microRNA targets. Cell *120*, 15–20.

McNeill, E., and Van Vactor, D. (2012). MicroRNAs shape the neuronal landscape. Neuron *75*, 363–379.

Mercuri, N.B., Bonci, A., Pisani, A., Calabresi, P., and Bernardi, G. (1995). Actions of glycine on non-dopaminergic neurons of the rat substantia nigra. Eur. J. Neurosci. *7*, 2351–2354.

Miñones-Moyano, E., Porta, S., Escaramís, G., Rabionet, R., Iraola, S., Kagerbauer, B., Espinosa-Parrilla, Y., Ferrer, I., Estivill, X., and Martí, E. (2011). MicroRNA profiling of Parkinson's disease brains identifies early downregulation of miR-34b/c which modulate mitochondrial function. Hum. Mol. Genet. *20*, 3067–3078.

Navarro, F., and Lieberman, J. (2015). miR-34 and p53: new insights into a complex functional relationship. PLoS One *10*, e0132767.

Nouri, N., Patel, M.J., Joksimovic, M., Poulin, J.F., Anderegg, A., Taketo, M.M., Ma, Y.C., and Awatramani, R. (2015). Excessive Wnt/beta-catenin signaling promotes midbrain floor plate neurogenesis, but results in vacillating dopamine progenitors. Mol. Cell. Neurosci. *68*, 131–142.

Rheinbay, E., Suvà, M.L., Gillespie, S.M., Wakimoto, H., Patel, A.P., Shahid, M., Oksuz, O., Rabkin, S.D., Martuza, R.L., Rivera, M.N., et al. (2013). An aberrant transcription factor network essential

for wnt signaling and stem cell maintenance in glioblastoma. Cell Rep. *3*, 1567–1579.

Saba, R., Storchel, P.H., Aksoy-Aksel, A., Kepura, F., Lippi, G., Plant, T.D., and Schratt, G.M. (2012). Dopamine-regulated microRNA MiR-181a controls GluA2 surface expression in hippocampal neurons. Mol. Cell. Biol. *32*, 619–632.

Sawamoto, K., Nakao, N., Kobayashi, K., Matsushita, N., Takahashi, H., Kakishita, K., Yamamoto, A., Yoshizaki, T., Terashima, T., Murakami, F., et al. (2001). Visualization, direct isolation, and transplantation of midbrain dopaminergic neurons. Proc. Natl. Acad. Sci. USA *98*, 6423–6428.

Stark, A., Brennecke, J., Bushati, N., Russell, R.B., and Cohen, S.M. (2005). Animal MicroRNAs confer robustness to gene expression and have a significant impact on 3′UTR evolution. Cell *123*, 1133–1146.

Subramanyam, D., Lamouille, S., Judson, R.L., Liu, J.Y., Bucay, N., Derynck, R., and Blelloch, R. (2011). Multiple targets of miR-302 and miR-372 promote reprogramming of human fibroblasts to induced pluripotent stem cells. Nat. Biotech. *29*, 443–448.

Tan, C.L., Plotkin, J.L., Veno, M.T., von Schimmelmann, M., Feinberg, P., Mann, S., Handler, A., Kjems, J., Surmeier, D.J., O'Carroll, D., et al. (2013). MicroRNA-128 governs neuronal excitability and motor behavior in mice. Science *342*, 1254–1258.

Tobon, K.E., Chang, D., and Kuzhikandathil, E.V. (2012). MicroRNA 142-3p mediates post-transcriptional regulation of D1 dopamine receptor expression. PLoS One *7*, e49288.

Victor, M.B., Richner, M., Hermanstyne, T.O., Ransdell, J.L., Sobieski, C., Deng, P.Y., Klyachko, V.A., Nerbonne, J.M., and Yoo, A.S. (2014). Generation of human striatal neurons by MicroRNA-dependent direct conversion of fibroblasts. Neuron *84*, 311–323.

Vierbuchen, T., Ostermeier, A., Pang, Z.P., Kokubu, Y., Südhof, T.C., and Wernig, M. (2010). Direct conversion of fibroblasts to functional neurons by defined factors. Nature *463*, 1035–1041.

Yang, D., Li, T., Wang, Y., Tang, Y., Cui, H., Tang, Y., Zhang, X., Chen, D., Shen, N., and Le, W. (2012). miR-132 regulates the differentiation of dopamine neurons by directly targeting Nurr1 expression. J. Cell Sci. *125*, 1673–1682.

Yoo, A.S., Sun, A.X., Li, L., Shcheglovitov, A., Portmann, T., Li, Y., Lee-Messer, C., Dolmetsch, R.E., Tsien, R.W., and Crabtree, G.R. (2011). MicroRNA-mediated conversion of human fibroblasts to neurons. Nature *476*, 228–231.

Zhao, S., Maxwell, S., Jimenez-Beristain, A., Vives, J., Kuehner, E., Zhao, J., O'Brien, C., de Felipe, C., Semina, E., and Li, M. (2004). Generation of embryonic stem cells and transgenic mice expressing green fluorescence protein in midbrain dopaminergic neurons. Eur. J. Neurosci. *19*, 1133–1140.